We are IntechOpen,
the world's leading publisher of Open Access books
Built by scientists, for scientists

6,900
Open access books available

186,000
International authors and editors

200M
Downloads

Our authors are among the

154
Countries delivered to

TOP 1%
most cited scientists

12.2%
Contributors from top 500 universities

CLARIVATE ANALYTICS
BOOK CITATION INDEX
INDEXED

WEB OF SCIENCE™

Selection of our books indexed in the Book Citation Index
in Web of Science™ Core Collection (BKCI)

Interested in publishing with us?
Contact book.department@intechopen.com

Numbers displayed above are based on latest data collected.
For more information visit www.intechopen.com

Localized and Propagated Surface Plasmons in Metal Nanoparticles and Nanowires

Xianguang Yang and Baojun Li

Additional information is available at the end of the chapter

Abstract

Surface plasmons are coherent electron oscillations behaving as localized and propagated modes in metal nanoparticles and nanowires, respectively. In this chapter, we first review some of the applications made in plasmonics with gold nanorods/nanospheres and silver nanowires. For gold nanoparticles with a size of 1–100 nm, the surface plasmons are confined around the particle surface as localized modes to enhance the near-field. For diameter of around 200–300 nm silver nanowires with a length up to 10 μm, the surface plasmons can propagate along the nanowires as waveguide modes to guide the plasmons. We then describe some novel results with regarding to gold nanorod enhanced light emission, silver nanowire supported plasmonic waveguide, gold nanosphere mediated whispering-gallery-mode emission, and energy conversion in silver-polymer plasmonic nanostructures. The work of this chapter highlights the applications of metal nanoparticles and nanowires in plasmonic waveguides to achieve optical energy generation, propagation, and conversion.

Keywords: surface plasmon waveguides, metal nanoparticles, nanowires, nanostructures, absorption

1. Introduction

Plasmonics has the fascinating ability to localize and guide light wave at the deep sub-wavelength scale, becomes an inter-discipline merging photonics with electronics [1–6]. Surface plasmons are free electron oscillations induced by optical methods at the metal surfaces. Both localized and propagated surface plasmons excited in metal nanoparticles and nanowires are of great interest. They not only break the diffraction limit but also allow

to guide light in various geometries such as 90° bending [1]. This promises the scaling of optical devices down to the diffraction limit for miniaturized photonic circuits. The localized surface plasmons have the functionality to scatter, absorb and squeeze light into nanometer scale, providing large enhancements of local near-fields [7]. It holds the potential applications in data storage, light energy generation, sub-wavelength optics, nano-optical tweezers, biophotonics and nanoscopy [8–11]. Gold nanoparticles with sphere/rod shapes and size below 100 nm are highly investigated for many useful applications, such as non/radiative enhancement of nano-crystals [12], inter-particle coupling effect [13], single particle plasmon spectroscopy [14–16], plasmonic sensing [17–19], plasmonic photocatalysis [20–22], and so on. Different from the localized surface plasmons of individual nanoparticles, the propagated surface plasmons existing at flat/curved surfaces in metallic planes, films, and wires also exhibit intriguing plasmonic phenomena [23]. The propagation length of surface plasmon modes is inevitably limited by metallic absorption, could also be strongly confined in the lateral section normal to propagation direction. This implies that plasmonic waveguides could transport larger bandwidth of information than that of conventional photonic waveguides. However, there is a trade-off between propagation loss and mode confinement in plasmonic waveguides [24]. To balance this trade off, an alternative method by seamlessly integrating photonic waveguides into plasmonic waveguides can be used [25]. Silver nanowires usually act as plasmonic waveguides with lateral size of 200–300 nm and axial length up to 10 μm, exhibiting many interesting applications. For example, plasmonic interference [26], wave-particle duality [27], remote excitation of Raman scattering [28–30], long-distance plasmonic gain [31–33], broadside nano-antennas [34], etc. It is impossible to introduce every result on plasmonics in this short chapter. In the following sections, we will specifically describe some novel results with gold nanorods/nanospheres and silver nanowires for achieving optical energy generation, propagation, and conversion.

2. Localized surface plasmon in gold nanorods

Metal-enhanced fluorescence can be realized via the resonant coupling with localized surface plasmon in metallic nanoparticles, nanorods, and nanostructures [35–40]. Different form two-dimensional films and/or three-dimensional solutions, metal-enhanced fluorescence in one-dimensional waveguides could provide a lower power consumption and higher density integration for plasmonic circuits. Herein, we describe a novel result of gold nanorod enhanced light emission, which is realized by embedding gold nanorods into polymer photonic waveguide doped with quantum dots at low concentration.

To study plasmonic properties, a single plasmonic waveguide was placed on MgF_2 substrate with refractive index (n) of 1.39. A blue light at 473-nm wavelength was coupled into the plasmonic waveguide via evanescent field. **Figure 1a** shows the dark-field optical microscope image with red emission excited by the incident light at an optical power (P_{in}) of 0.1 μW, where positions A to E manifesting gold nanorod enhanced light emission from embedded quantum dots for representative measurements. To make a comparison, a single photonic waveguide has a similar diameter as that of the plasmonic waveguide, was also excited by the incident light at an optical power (P_{in}) of 0.1 μW (**Figure 1b**).
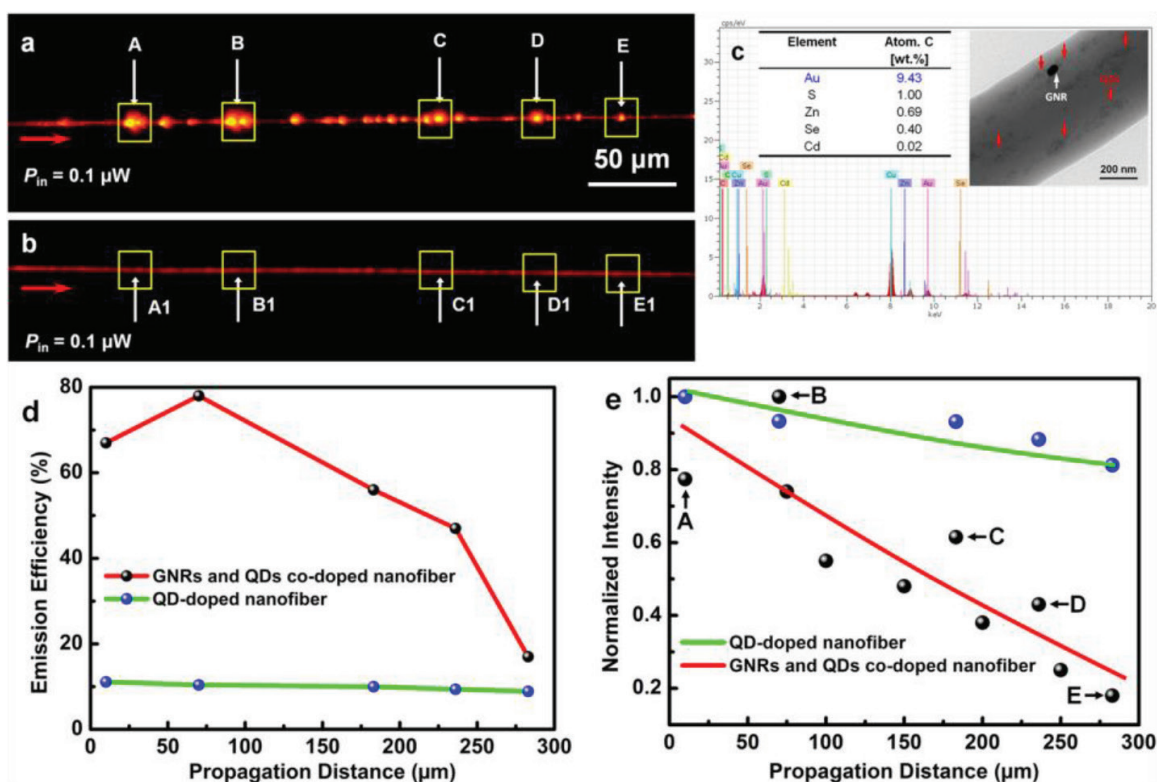
Figure 1. Plasmonic waveguides in polymer embedded with gold nanorods. Dark-field optical microscope images are corresponding to (a) plasmonic waveguide with gold nanorods and (b) photonic waveguide without gold nanorods. (c) TEM and EDS analysis of a plasmonic waveguide. (d) The relationship between emission efficiency and propagation distance. (e) Dependence of normalized intensity on the propagation distance. Red curve is for plasmonic waveguide, while blue curve is for photonic waveguide. GNRs mean gold nanorods, and QDs mean quantum dots. Reprinted with permission [41].

To clearly examine the distributions of gold nanorods and quantum dots embedded in the plasmonic waveguide, both a bright-field transmission electron microscope (TEM) and an energy dispersive X-ray spectroscopy (EDS) were simultaneously performed. **Figure 1c** shows EDS spectrum of a plasmonic waveguide while the inset shows the corresponding TEM image. The EDS spectrum verifies the existence of Au (9.43 wt%), Cd (0.02 wt%), Se (0.40 wt%), Zn (0.69 wt%), and S (1.00 wt%) elements. They came from gold nanorods and CdSe-ZnS core-shell quantum dots. The embedded concentrations for gold nanorods and quantum dots are estimated to be of 4 μm^{-3} and 3.2×10^3 μm^{-3}, respectively.

Figure 1d shows the light emission efficiency at positions A to E (with gold nanorods) and positions A1 to E1 (without gold nanorods). At position B, the emission enhancement is maximized, where plasmonic wavelength overlapped with emission wavelength of quantum dots [42]. The mechanism for emission enhancement can be interpreted as follows: (1) by coupling a 473-nm blue light into plasmonic waveguide, the embedded quantum dots are photoexcited and then emit 600-nm red light. (2) The emitted 600-nm red light excites the localized surface plasmon of gold nanorods, which leads to an enhancement of local near-field. (3) The enhanced local near-field increases the stimulated radiative decay rate of quantum dots, thus leading to the increasing of quantum yields and the decreasing of fluorescence lifetime [43].

In fact, emission quenching could happen because free electrons can transfer from quantum dots to gold nanorods once they are closely contacted. For instance, emission quenching of quantum dots by gold nanoparticles has been previously reported [44, 45]. As shown in **Figure 1a**, the locally enhanced inhomogenously distributed emission spots can be explained by the unevenly-increased in the local density of plasmonic sates around gold nanorods. This inhomogeneous can be improved by linking quantum dots and gold nanorods via chemical/biological coupling to ensure their efficient interactions. In any case, the total emission efficiency depends on the quantum yield, self-absorption of quantum dots, resonance properties of localized surface plasmon in gold nanorods, and propagation loss of the plasmonic waveguide.

For the measurements of emission intensity, the dark-field optical microscope images with RGB modes were transformed into gray levels employing software (Adobe Photoshop), and the gray values were summed up to acquire the normalized intensity, this method was previously reported [46]. The yellow rectangular in **Figure 1a** and **b** is taken as the sum-up region with an area of 21×18 μm^2. **Figure 1e** shows the normalized intensity of red emission along the plasmonic waveguide (red line) and photonic waveguide (green line) as a function of propagation distance. It indicates that the existence of gold nanorods seriously affects the propagation distance of plasmonic waveguide, which is due to the larger scattering loss. In addition, some local regions with non-uniform particle density, refractive index, and crystalline would give rise to bulk scattering in the plasmonic waveguide.

3. Propagated surface plasmon in silver nanowires

Silver nanowires possess sub-wavelength mode confinement and low propagation loss, but the couple of light into such small nanowires are extremely challengeable. For this challenge, several methods to light coupling have been proposed, including: (1) total internal reflection method utilizing an optical prism to compensate for momentum mismatch between photon and surface plasmon [47]; (2) localized excitation method via focusing laser beam directly on a scattering center of silver nanowires [48, 49]; and (3) near-field coupling method using optical dipole with large momentum components to match that of surface plasmon, where quantum emitters usually located in the near-field of silver nanowire [50, 51]. However, above three coupling methods cannot easily interconnect silver nanowires with photonic waveguides for nanophotonic circuits. Herein, we describe a novel result of silver nanowire supported plasmonic waveguide by coupling photons from quantum-dot-doped nanowire.

A scanning electron microscope (SEM) micrograph of one silver nanowire with a diameter of 300 nm was interconnected with a quantum-dot-doped nanowire with a diameter of 800 nm at an angle of 60° is presented in **Figure 2a**. To inspect this crossing angle in better detail, an enlarged view is given in **Figure 2b**. For more practical device applications, the interconnection of more than one silver nanowire with a same quantum-dot-doped polymer nanowire is extremely desirable. For example, **Figure 2c** presents an SEM micrograph of silver nanowires 1 and 2 with the same diameters of 300 nm were interconnected with a quantum-dot-doped nanowire (800-nm in diameter) at angles of 60 and 65°, respectively. The mutual distance between silver nanowires 1 and 2 is about 6.4 μm. To realize hybrid interconnection with high-density of plasmonic and photonic nanowires, more than three silver plasmonic nanowires
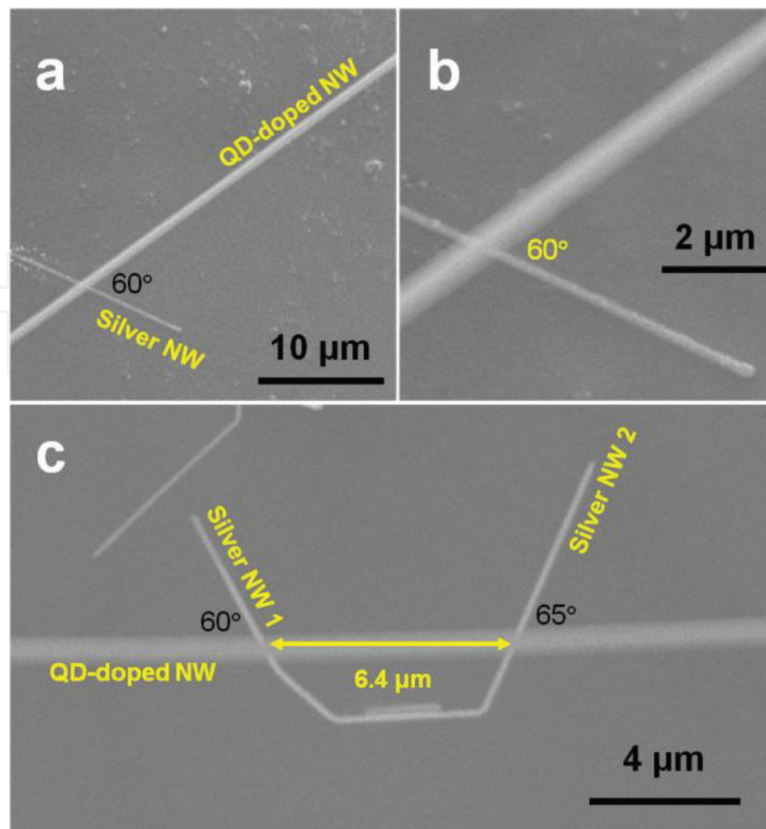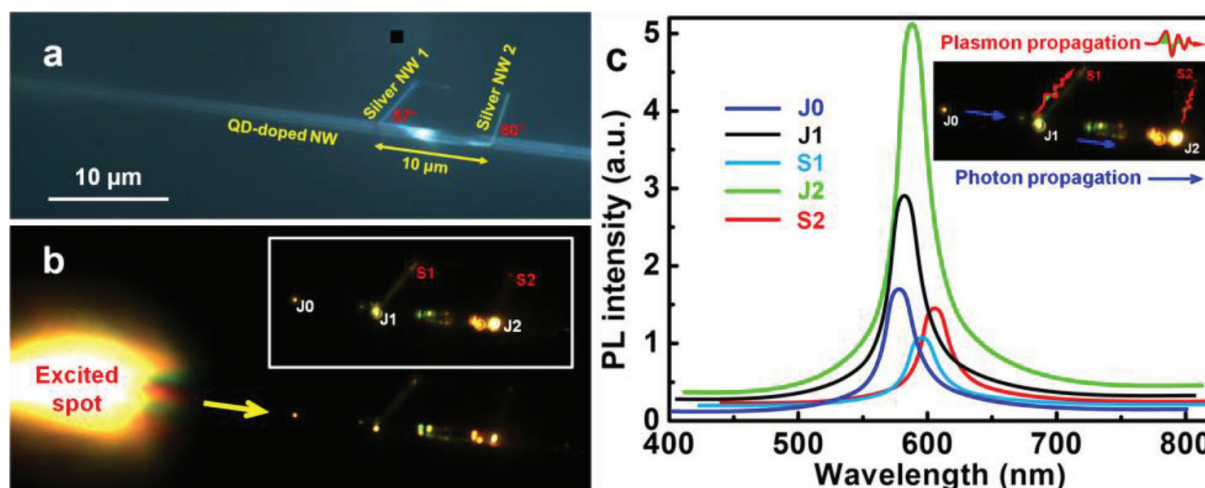
Figure 2. SEM characterization of silver nanowires. (a) One silver nanowire was interconnected with a quantum-dot-doped nanowire at an angle of 60°. (b) Enlarged view of the crossing angle in (a). (c) Silver nanowires 1 and 2 were interconnected with the same quantum-dot-doped nanowire at crossing angles of 60 and 65°, respectively. Note: NW means nanowire, and QD means quantum dot. Reprinted with permission [54].

with distinct lengths and diameters would be interconnected with the same quantum-dot-doped photonic nanowire at distinct angles and intervals, which could provide versatile multi-functionalities in nanoscale circuits [52, 53].

Optical characterization of the silver nanowires was performed under an optical microscopy using a micro-spectrophotometer (CRAIC, 20/20 PV, USA). **Figure 3a** shows a reflection-type optical microscope image of silver nanowires 1 and 2 with the same diameters of 300 nm was interconnected with an 800-nm diameter quantum-dot-doped nanowire at angles of 57 and 80°, respectively. The lengths of silver nanowires 1 and 2 are about 5 and 4 μm, respectively, and the mutual distance between them is of 10 μm. **Figure 3b** gives a scattering-type micrograph under dark-field for the crossing structure in **Figure 3a** illuminated by a beam of 532-nm laser at an optical power of 10 mW. The scattering position J0 comes from individual defects in the quantum-dot-doped nanowire. The larger scattering positions J1 and J2 come from the photonic-plasmonic junctions formed with the silver and quantum-dot-doped nanowires [55]. In the photonic-plasmonic junctions, when the surface plasmon of silver nanowires were launched by photoluminescence from quantum-dot-doped nanowire. Among the launched plasmonic modes, the dominant mode is longitudinal mode and the produced resonance could have Fabry-Perot characteristics [56]. The smaller scattering positions S1 and S2 come from the end tips of the silver nanowires, where the propagated surface plasmons were converted into free space photons.

The two silver nanowires with same diameters of 300 nm can strongly confine the 580-nm photoluminescence into sub-wavelength scale dimensions, giving rise to their relatively compact interconnection with the quantum-dot-doped nanowire. For briefness, the photoluminescence spectra collected at positions J0, J1, J2, S1, and S2 were plotted in a single graph as **Figure 3c**. The peak wavelengths for positions J0, J1, J2, S1, and S2 are 580, 585, 590, 595, and 605 nm, respectively. The inset image of **Figure 3c** shows surface plasmon propagation in the silver nanowires and emitted photon propagation in the quantum-dot-doped polymer nanowire. The quantum-dot-doped nanowire produced distinct colors of yellow, yellow-orange, and orange from positions J0, J1, and J2, respectively. This phenomenon is called "wavelength-converted waveguiding", which also previously observed in dye-doped polymer nanofiber [57]. The color difference between yellow-orange (J1) and red-orange (S1) in silver nanowire 1 comes from the metallic loss induced energy dissipation, and the resulted peak wavelength changed from 585 to 595 nm. Similarly, the colors are different between orange (J2) and red (S2) in silver nanowire 2, and the peak wavelength changed from 590 to 605 nm. This is a frequency-dependent dispersion effect in these two silver nanowires [58].

Another novel result is optical routing in single silver nanowires [59]. Semiconductor micro-ribbon and silver nanowires were assembled to realize routing structure, as shown in SEM micrograph of **Figure 4a**. One silver nanowire was sitting on top of a semiconductor SnO_2 ribbon, and a second silver nanowire just cling to it with a 12 μm overlapping. The three color arrows show the end tips of the silver nanowires, and the Inset shows the enlarged view of the overlapping region. The surfactants on the silver nanowires have already been cleared so that the two silver nanowires were contact directly. **Figure 4b** and **c** show the intensity mapping and real-color micrograph of the optical routing from semiconductor SnO_2 ribbon

Figure 3. Optical characterization of silver nanowires. (a) Reflection-type optical microscope image of silver nanowires 1 and 2 were interconnected with the same quantum-dot-doped nanowire at crossing angles of 57 and 80°, respectively. Note that the black box (area: 1 μm²) near silver nanowire 1 is the sampling spot to spectrum measuring. (b) Scattering-type optical microscope image of the crossing structure in (a) was illuminated by a 532-nm excitation laser with a spot diameter of 15 μm at an optical power of 10 mW. The yellow arrow gives the propagation direction of excited 580-nm photoluminescence. Inset was captured by focalizing to the two silver nanowires and measures the photoluminescence spectra on positions J0, J1, J2, S1, and S2. The scale bar in (a) is applicable to (b). (c) Photoluminescence spectra measured at positions J0, J1, J2, S1, and S2. Inset shows the propagation of photons and plasmons. NW means nanowire, and QD means quantum dot. PL means photoluminescence. Reprinted with permission [54].
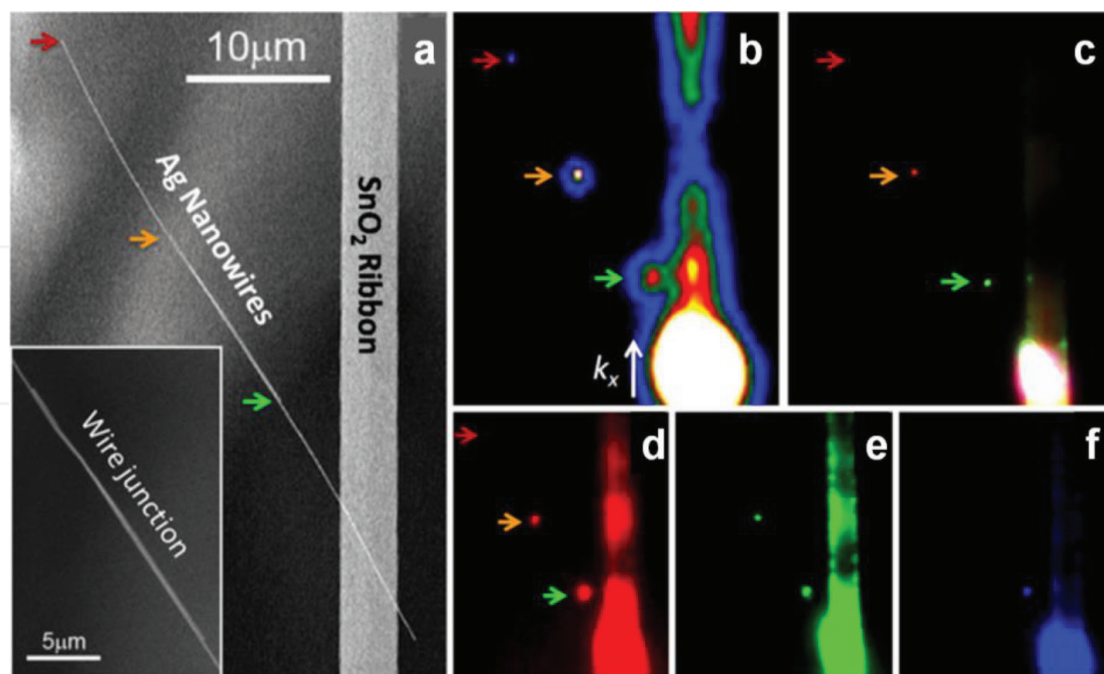
Figure 4. Optical routing of silver nanowires. (a) SEM micrograph of two overlapped silver nanowires coupling to a SnO$_2$ ribbon. The length of overlapped region is 12 μm. (inset) overlapped region of the two silver nanowires. (b) Intensity mapping of the routing structure when the photoluminescence of the SnO$_2$ ribbon was launched and coupled into silver nanowires with three different emission spots at distal ends. (c) the real-color micrograph of the same view as in (b). (d–f) individual red (R), green (G), and blue (B) color channels from (c), giving a gradual decrease in propagation loss from short (f) to long (d) wavelengths. The colors are obtained with the Bayer filter from the CoolSnap. Reprinted with permission [59].

photoluminescence. Surface plasmons were launched into the first silver nanowire in the silver-SnO$_2$ overlapped region, and evanescently coupled into the second silver nanowire with low scattering loss in the silver-silver overlapped region. This efficient coupling in the silver-silver region is benefited from the large surface plasmon mode overlaps due to the closely contact between the nanowires. Interestingly, the relationship of the end tip emission color with propagation distance on the case of single silver nanowire was also investigated. **Figure 4d–4f** individually display the red, green, and blue color panel of the real-color micrograph in **Figure 4c**. The closer the propagation distance, the emission composes more short-wavelength components. The blue-wavelength components just exist at the first silver nanowire tip with a propagation distance of 8 μm, while the green-wavelength components survived 20 μm of propagation and the red-wavelength components were the only visible one with propagation distance up to 40 μm.

4. Plasmonic nano-cavity in gold nanospheres

Different from dielectric micro-cavities, plasmonic nano-cavities could confine light into the nanometer scale mode volume [60, 61]. Optical investigations based on circular nano-cavities are extremely interesting due to the whispering-gallery-modes, which are attributed to the total internal reflection of light at the plasmonic interface along the equator. Herein, we describe

a novel result of whispering-gallery-mode emission in plasmonic nano-cavity, which combines gold nanosphere and quantum dots by using electrostatic attraction. **Figure 5a** shows polarization-dependent photoluminescence intensity of the emitted light. The dependence can be described by a sinusoidal function. The minimum (−90°) and the maximum (10°) photoluminescence intensities are corresponding to perpendicular and parallel to the extinction direction of the gold nanosphere, respectively. The period of 180° is similar to that reported in quantum dots on gold nanodiscs [62].

Figure 5b shows the emission spectrum containing five narrow bands, which indicates the characteristic of the whispering-gallery-modes. The maximum peak of whispering-gallery-mode is well coincidence with that of solution photoluminescence. Meanwhile, the optical feedback is strong enough to resist the plasmonic loss. **Figure 5c** shows the photoluminescence spectra of 800 and 550 nm diameter quantum-dot-coated gold nanosphere producing the several narrow bands, while the maximum peaks towards to short wavelength range as diameter increasing. This phenomenon is governed by changing in whispering-gallery-mode
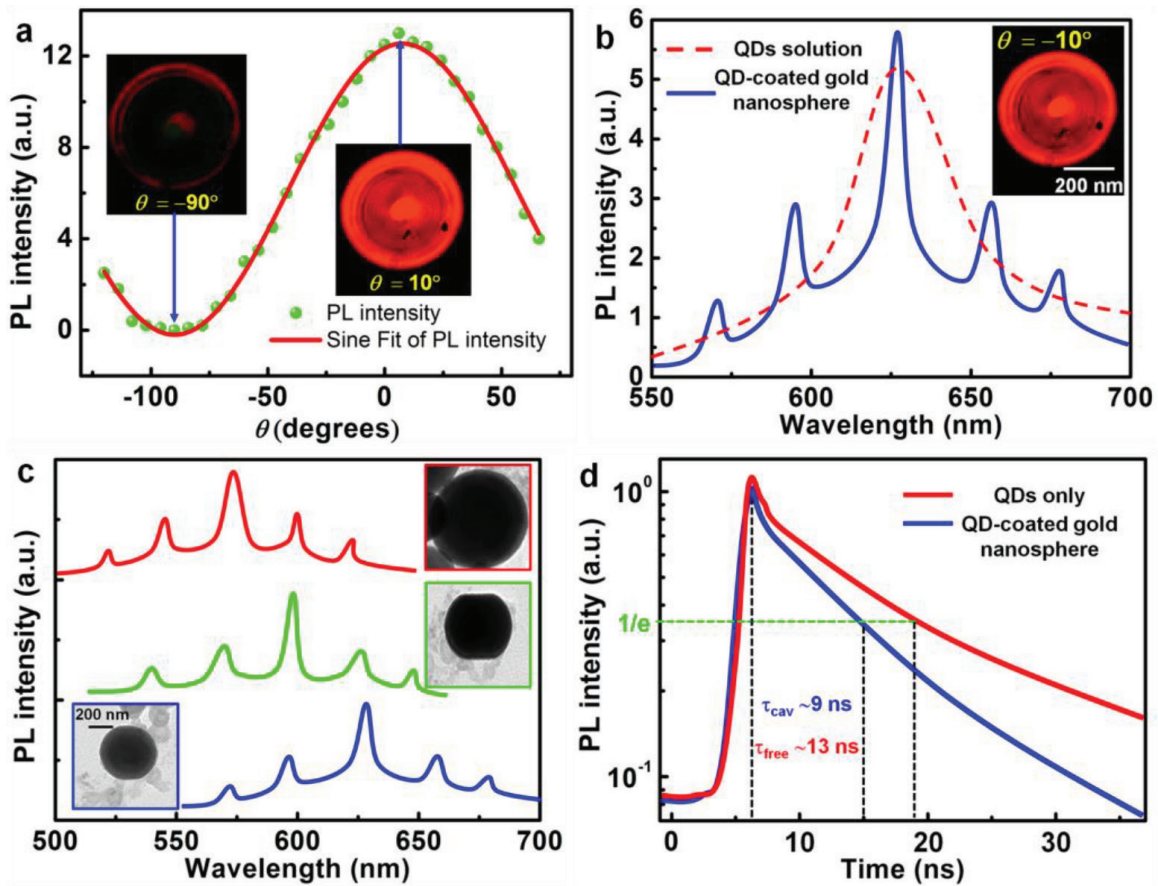

Figure 5. Whispering-gallery-mode emission. (a) Photoluminescence intensity as a function of polarization angle. Insets show optical micrographs of quantum-dot-coated gold nanosphere with polarization angles of 90 and 10°. (b) Whispering-gallery-mode emission spectrum from a quantum-dot-coated gold nanosphere (solid blue line) and the quantum dots solution emission spectrum (dashed red line). (c) Whispering-gallery-mode emission spectra of quantum-dot-coated gold nanosphere with diameters of 490 nm (blue), 550 nm (green), and 800 nm (red). Insets: Corresponding TEM micrographs. (d) Photoluminescence decay spectra of quantum-dot-coated gold nanosphere (blue line) and the quantum dots solution (red line) with lifetime at 9 and 13 ns, respectively. Reprinted with permission [63].

states density and the near-field coupling strengths. **Figure 5d** shows the photoluminescence decay spectra of quantum-dot-coated gold nanosphere (blue) and the quantum dots solution (red). They are multiple-exponential process, including intrinsic decay, plasmonic quenching, and plasmonic enhancement. The lifetimes were calculated from $1/e$ values to be of 9 and 13 ns, respectively. The decrease in lifetime verifies the near-field coupling between the localized surface plasmon of gold nanosphere and the radiative decay of quantum dots. As the light waves were confined along the equator of gold nanosphere by localized surface plasmon, the propagation medium of the light waves are the coated layers with quantum dots.

Molecular emitters located in a plasmonic nano-cavity experience an intriguing process to be coupled into the surrounding optical field [64]. Cucurbit(7)uril is hydro-soluble and can encapsulate only one molecule of methylene-blue inside it. Encapsulation of methylene-blue inside cucurbit(7)uril is verified by absorption spectroscopy analysis (**Figure 6a**): methylene-blue dimmers (with characteristic 'shoulder' of small peak at 625 nm on the red solid curve) disappear when mixing low concentrations of methylene-blue into cucurbit(7)uril (**Figure 6a**, blue solid curve). Contrast experiments use the smaller molecule of cucurbit(5)uril also have this shoulder peak (red dashed curve), eliminating the possibility of parasitic binding. Encapsulating single molecules of methylene-blue into cucurbit(7)uril can be used to avoid molecular aggregation. Carboxide portals at either end of the 0.9-nm in height cucurbit(n)uril molecules with rims were binding flatly onto the gold surface (**Figure 6b**). The formed nano-cavity volume can be down to less than 40 nm³. This decorating of molecules via light opens up the venue to manipulate chemical bonds [65].
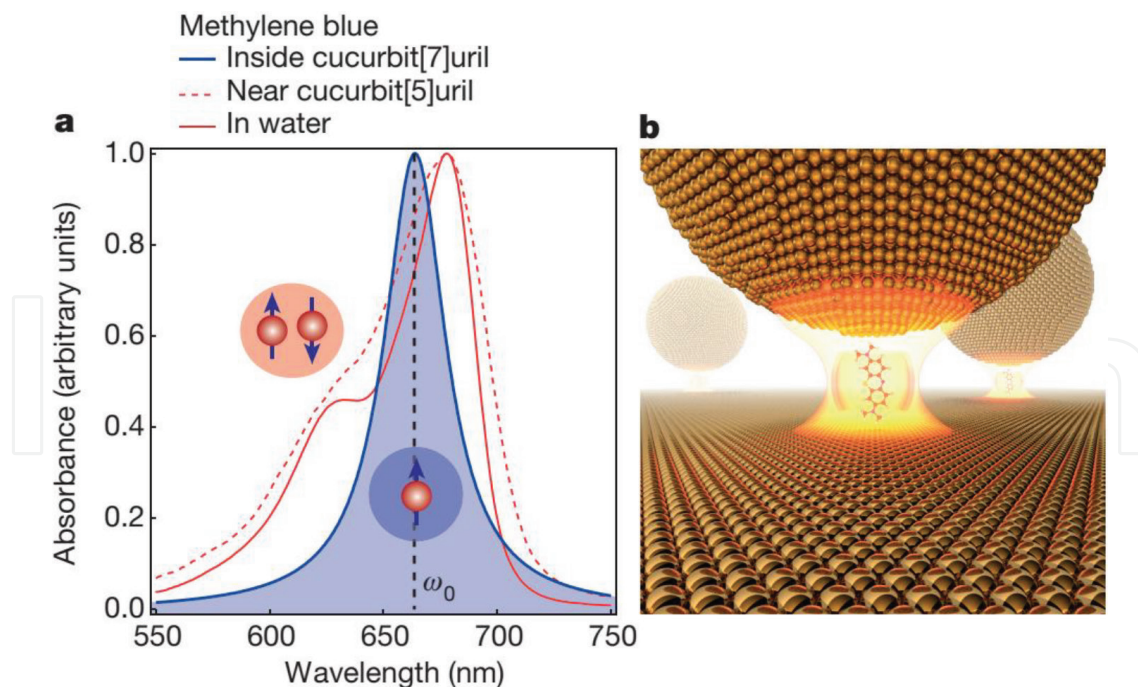
Figure 6. Plasmonic nano-cavity with a single dye molecule. (a) Absorption spectra for methylene-blue in water, with (blue solid line) and without (red solid line) encapsulation in cucurbit(n)urils. Blue and red icons show individual molecules (centred at ω_0) and paired molecular dimmers, respectively. (b) Schematic illustration of a methylene-blue molecule in cucurbit(n)uril, located within the gold nanosphere-on-mirror geometry configuration. Reprinted with permission [64].
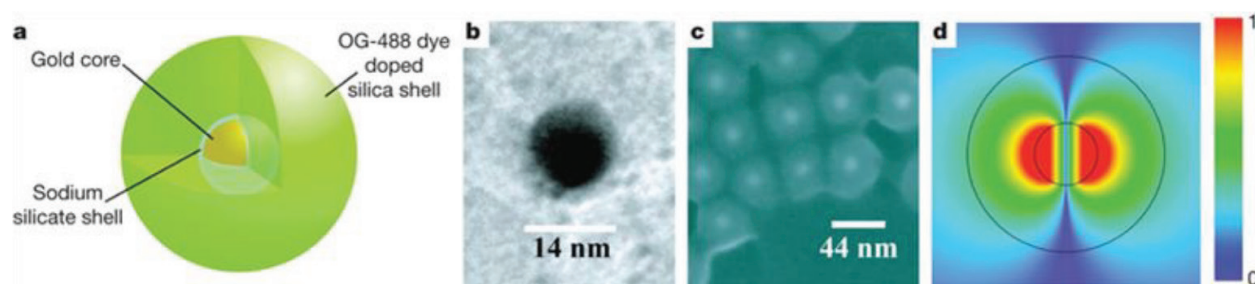
Figure 7. Plasmonic nano-cavity design. (a) Schematic of the hybrid nanosphere, indicating silica shell doped with dye molecules. (b) TEM micrograph of gold core. (c) SEM micrograph of gold-silica-dye core-shell nanospheres. (d) Localized surface plasmon laser mode with λ of 525 nm and Q factor of 14.8. The outer and inner circles stand for the 44-nm shell and 14-nm core, respectively. Strength color bar is on the right. Reprinted with permission [66].

Another novel result shows that 44-nm in diameter nanospheres with a gold core and dye-doped silica shell can be used to overcome the plasmonic loss with optical gain and realize a stimulated emission of surface plasmons [66]. **Figure 7a** shows a nanosphere with a gold core, supporting for localized surface plasmon modes, and coated by a silica shell doped with organic dye OG-488 (Oregon Green 488), supporting for optical gain. TEM and SEM measurements show the diameter of gold core and the thickness of silica shell are about 14 and 15 nm, respectively (**Figure 7b** and **c**). The molecule number of dye per nanosphere was estimated to be about 2.7×10^3, and the nanosphere concentration in suspension was about 3×10^{11} cm^{-3}. The calculation of plasmonic laser mode (**Figure 7d**) obtains the stimulated emission wavelength (λ) to be of 525 nm and the quality (Q)-factor to be of 14.8. Although this Q-factor is governed by optical absorption, the produced gain is large enough to overcome the plasmonic loss.

5. Plasmonic conversion in silver-polymer nanostructures

Organic polymers with extraordinary properties to incorporate with laser dyes for providing optical gain over broadband visible spectrum, which makes them potential for tunable full-color lasers [67, 68]. Meanwhile, the mechanical flexibility of polymers allows to integrate them with metallic nanostructures, confining light into a small mode volume by surface plasmon [69]. In addition, flexible polymers have an outstanding function to self-assemble into optical micro-cavities with high-quality, where propagated light beam will be continuously confined via total internal reflection. Consequently, the large evanescent field around the air-cavity interface results in efficient conversion between photon and surface plasmon [70]. Herein, we describe a plasmonic conversion to obtain sub-wavelength output of full-color lasers in a silver-polymer heterostructure [71]. **Figure 8a** shows the assemble process of PS and dye molecules via dropping a defined amount of water into the PS-dye blend solution. During the nucleus formation of PS, the powerful π-π interaction makes the dye molecules slowly diffuse into the PS matrix. Once the solvent was evaporated, the silver-polymer microdisks with dyes can be successfully fabricated. Four organic dyes, trans-DPDSB, C153, CNDPASDB, and HMDMAC, with emission colors across the full visible spectrum, were intentionally selected for optical gain media. Under ultraviolet (330–380 nm) excitation, the silver-polymer micro-disks emitted homogenous blue (b), cyan (c), green-yellow (d), and red (e) colors, respectively
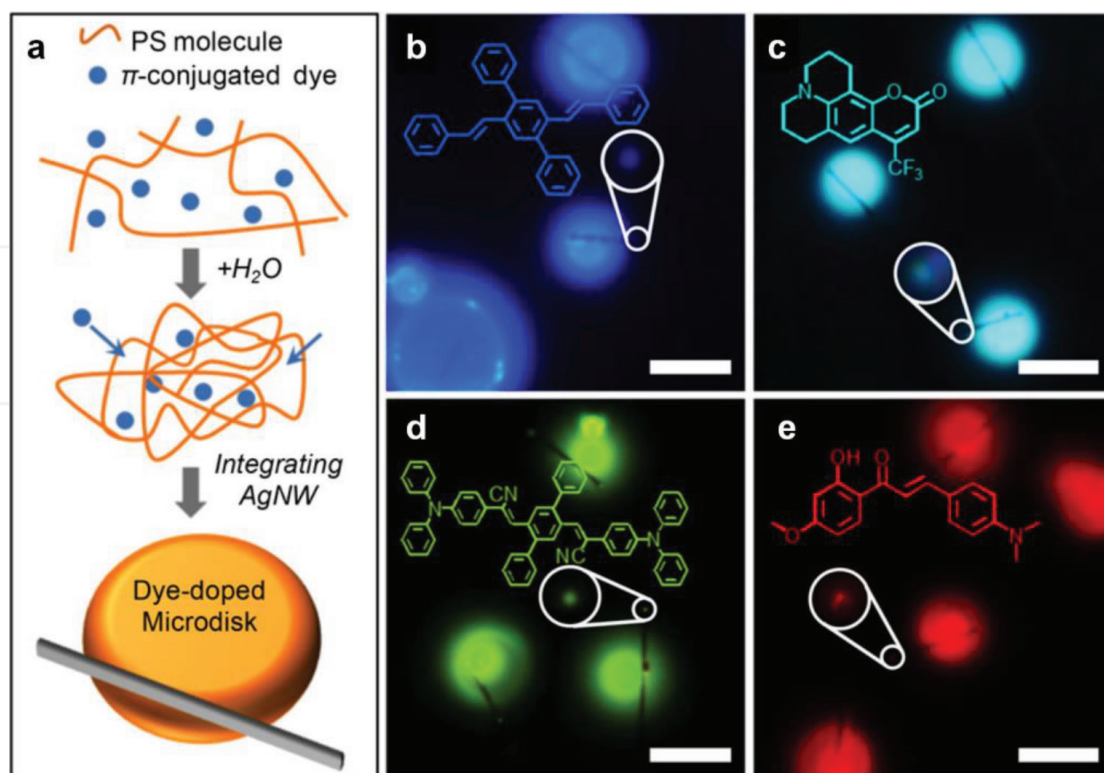
Figure 8. Sub-wavelength output of micro-lasers. (a) Diagram of the strategy to dope π-conjugated dye into microdisk for silver-polymer nanostructures. (b–e) Dark-field photoluminescence micrographs of the silver-polymer microdisks doped with organic dyes of (b) trans-DPDSB, (c) C153, (d) CNDPASDB, and (e) HMDMAC, respectively, under ultraviolet excitation. Photoluminescence spots enlarged in the white circles come from surface plasmon scattering in silver nanowire tips. Scale bar, 10 μm. Reprinted with permission [71].

(**Figure 8b–8e**). Importantly, the full colors were outputted with the sub-wavelength silver nanowire at end tips (white circles). This demonstrates the typical feature of surface plasmon waveguide, and the plasmonic conversion at the silver-polymer connections.

Another novel result of energy conversion between photonic nanowire and plasmonic nanowire will be described [72]. The photonic nanowire is CdSe-ZnS core-shell quantum dots doped polymer nanowire, and the silver nanowire served as plasmonic nanowire. The conversion efficiency is about 32%, which is realized by the Förster resonance energy transfer. **Figure 9a** shows SEM micrograph of quantum-dot-doped photonic nanowire were interconnected with silver plasmonic nanowire at a crossed angle of 45°. Once the plasmonic and photonic nanowires are directly contact, the surface plasmon field and evanescent field around photonic nanowire would overlap, leading to efficient conversion from photon to plasmon at the coupling area [73]. **Figure 9b** gives the dark-field optical micrograph of the silver-polymer crossed structure with red emission. The silver nanowire is about 55 μm in total length, and the lengths of the long (white arrow) and short (yellow arrow) regions on the two side of the photonic nanowire (refer as 'limbs') are 40 and 10 μm, respectively. The plasmonic conversion can be understood by the energy transition: photon-exciton-plasmon, and not need to match momentum, because the dipolar near-field of quantum dots has momentum components matching that of surface plasmon. Hence, the crossed angle cannot influence the plasmonic conversion efficiency [74]. The exponential decay curves of **Figure 9c** and **d** indicate surface
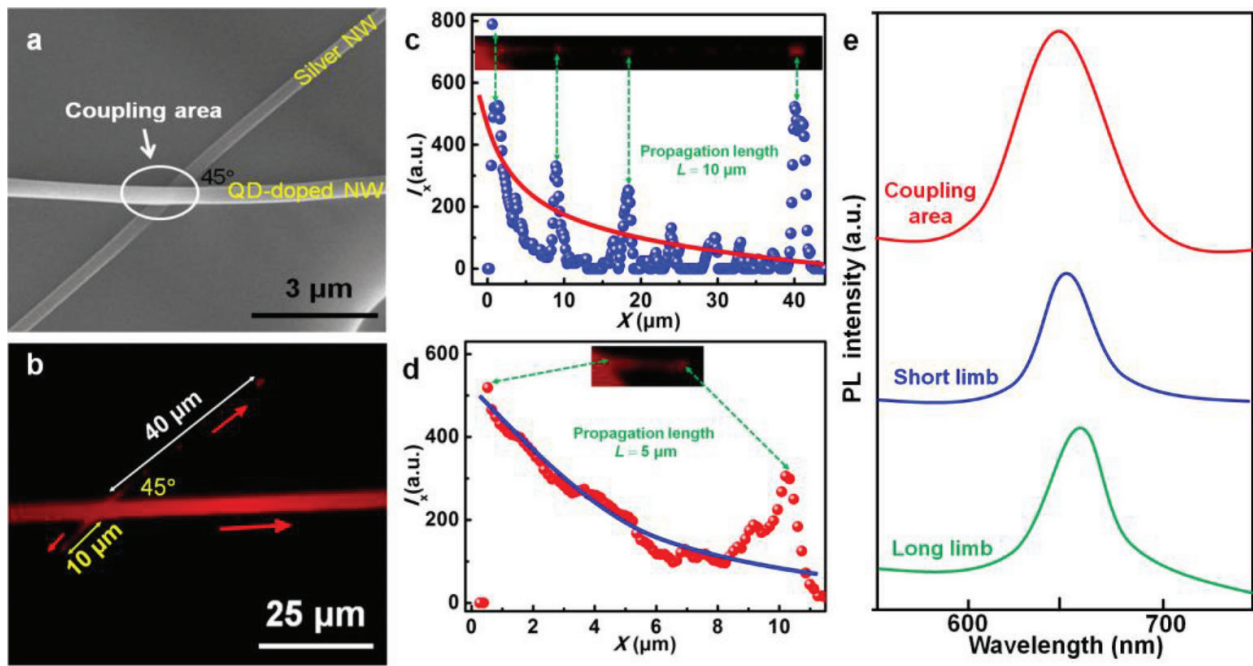
Figure 9. Energy conversion from photonic to plasmonic nanowires. (a) SEM micrograph of a 300-nm-diameter silver nanowire and a 400-nm-diameter quantum-dot-doped nanowire interconnected at a crossed angle of 45°. (b) Dark-field optical micrograph of the crossed silver-polymer structure excited by a 532-nm-wavelength laser at an optical power of 5 mW. (c, d) intensities of red emission along the long (c) and short (d) limbs of the silver plasmonic nanowire. Solid lines are plotted with an exponential decay. Insets and green dashed arrows give a visual guide. (e) Emission spectra collected at coupling area, two distal ends at long and short limbs. Reprinted with permission [72].

plasmon propagation lengths of 10 and 5 μm for long and short limbs, respectively. In addition, **Figure 9e** gives the emission spectra collected at coupling area, two distal ends of long and short limbs with wavelength centered at 650, 660, and 654 nm, respectively.

6. Conclusion

In this chapter, we have briefly introduced some important applications with localized and propagated surface plasmons in gold nanospheres/nanorods and silver nanowires. Specifically, we have described some novel results on gold nanorods enhanced light emission, surface plasmon propagation in silver nanowires, gold nanosphere as a plasmonic nano-cavity, energy conversion in silver-polymer nanostructures. Due to the limited space, many important progress in quantum plasmonics, nonlinear plasmonics, and photovoltaic plasmonics cannot be described altogether. The work in this chapter presents the applications of gold/silver nanoparticles/nanowires in nanophotonics to realize light generation, propagation, manipulation and conversion. It is an ultimate dream for plasmonics to combine photonics and electronics on practical devices and circuits. This huge challenge continued to motivate the research interests all around the world.

Acknowledgements

Conflict of interest

The authors declare no conflict of interest.

Author details

Xianguang Yang and Baojun Li*

*Address all correspondence to: baojunli@jnu.edu.cn

Institute of Nanophotonics, Jinan University, Guangzhou, China

References

[1] Maier SA, Brongersma ML, Kik PG, Meltzer S, Requicha AA, Atwater HA. Plasmonics—A route to nanoscale optical devices. Advanced Materials. 2001;**13**(19):1501-1505

[2] Polman A. Plasmonics applied. Science. 2008;**322**(5903):868-869

[3] Brongersma ML, Shalaev VM. The case for plasmonics. Science. 2010;**328**(5977):440-441

[4] Kauranen M, Zayats AV. Nonlinear plasmonics. Nature Photonics. 2012;**6**:737-748

[5] Marinica DC, Zapata M, Nordlander P, Kazansky AK, Echenique PM, Aizpurua J, Borisov AG. Active quantum plasmonics. Science Advances. 2015;**1**(11):e1501095

[6] Naldoni A, Shalaev VM, Brongersma ML. Applying plasmonics to a sustainable future. Science. 2017;**356**(6341):908-909

[7] Durach M, Rusina A, Stockman MI, Nelson K. Toward full spatiotemporal control on the nanoscale. Nano Letters. 2007;**7**(10):3145-3149

[8] Anker JN, Hall WP, Lyandres O, Shah NC, Zhao J, Van Duyne RP. Biosensing with plasmonic nanosensors. Nature Materials. 2008;**7**(6):442-453

[9] Schuller JA, Barnard ES, Cai W, Jun YC, White JS, Brongersma ML. Plasmonics for extreme light concentration and manipulation. Nature Materials. 2010;**9**(3):193-204

[10] Nicoletti O, de La Peña F, Leary RK, Holland DJ, Ducati C, Midgley PA. Three-dimensional imaging of localized surface plasmon resonances of metal nanoparticles. Nature. 2013; **502**(7469):80-84

[11] Juan ML, Righini M, Quidant R. Plasmon nano-optical tweezers. Nature Photonics. 2011; **5**(6):349-356

[12] Eustis S, El-Sayed MA. Why gold nanoparticles are more precious than pretty gold: Noble metal surface plasmon resonance and its enhancement of the radiative and nonradiative properties of nanocrystals of different shapes. Chemical Society Reviews. 2006;**35**(3):209-217

[13] Ghosh SK, Pal T. Interparticle coupling effect on the surface plasmon resonance of gold nanoparticles: From theory to applications. Chemical Reviews. 2007;**107**(11):4797-4862

[14] Tokareva I, Minko S, Fendler JH, Hutter E. Nanosensors based on responsive polymer brushes and gold nanoparticle enhanced transmission surface plasmon resonance spectroscopy. Journal of the American Chemical Society. 2004;**126**(49):15950-15951

[15] Novo C, Funston AM, Mulvaney P. Direct observation of chemical reactions on single gold nanocrystals using surface plasmon spectroscopy. Nature Nanotechnology. 2008; **3**(10):598-602

[16] Zijlstra P, Paulo PM, Orrit M. Optical detection of single non-absorbing molecules using the surface plasmon resonance of a gold nanorod. Nature Nanotechnology. 2012;**7**(6): 379-382

[17] Homola J. Surface plasmon resonance sensors for detection of chemical and biological species. Chemical Reviews. 2008;**108**(2):462-493

[18] Mayer KM, Hafner JH. Localized surface plasmon resonance sensors. Chemical Reviews. 2011;**111**(6):3828-3857

[19] Zeng S, Baillargeat D, Ho H-P, Yong K-T. Nanomaterials enhanced surface plasmon resonance for biological and chemical sensing applications. Chemical Society Reviews. 2014;**43**(10):3426-3452

[20] Murdoch M, Waterhouse G, Nadeem M, Metson J, Keane M, Howe R, Llorca J, Idriss H. The effect of gold loading and particle size on photocatalytic hydrogen production from ethanol over Au/TiO$_2$ nanoparticles. Nature Chemistry. 2011;**3**(6):489-492

[21] Hou W, Cronin SB. A review of surface plasmon resonance-enhanced photocatalysis. Advanced Functional Materials. 2013;**23**(13):1612-1619

[22] Lou Z, Kim S, Fujitsuka M, Yang X, Li B, Majima T. Anisotropic Ag$_2$S–Au triangular nanoprisms with desired configuration for plasmonic photocatalytic hydrogen generation in visible/near-infrared region. Advanced Functional Materials. 2018;**28**(13):1706969

[23] Han Z, Bozhevolnyi SI. Radiation guiding with surface plasmon polaritons. Reports on Progress in Physics. 2012;**76**(1):016402

[24] Gramotnev DK, Bozhevolnyi SI. Plasmonics beyond the diffraction limit. Nature Photonics. 2010;**4**(2):83-91

[25] Briggs RM, Grandidier J, Burgos SP, Feigenbaum E, Atwater HA. Efficient coupling between dielectric-loaded plasmonic and silicon photonic waveguides. Nano Letters. 2010;**10**(12):4851-4857

[26] Allione M, Temnov VV, Fedutik Y, Woggon U, Artemyev MV. Surface plasmon mediated interference phenomena in low-Q silver nanowire cavities. Nano Letters. 2008;**8**(1):31-35

[27] Kolesov R, Grotz B, Balasubramanian G, Stöhr RJ, Nicolet AA, Hemmer PR, Jelezko F, Wrachtrup J. Wave–particle duality of single surface plasmon polaritons. Nature Physics. 2009;**5**(7):470-474

[28] Fang Y, Wei H, Hao F, Nordlander P, Xu H. Remote-excitation surface-enhanced Raman scattering using propagating Ag nanowire plasmons. Nano Letters. 2009;**9**(5):2049-2053

[29] Sun M, Zhang Z, Wang P, Li Q, Ma F, Xu H. Remotely excited Raman optical activity using chiral plasmon propagation in Ag nanowires. Light: Science & Applications. 2013;**2**(11): e112

[30] Huang Y, Fang Y, Zhang Z, Zhu L, Sun M. Nanowire-supported plasmonic waveguide for remote excitation of surface-enhanced Raman scattering. Light: Science & Applications. 2014;**3**(8):e199

[31] Paul A, Zhen Y-R, Wang Y, Chang W-S, Xia Y, Nordlander P, Link S. Dye-assisted gain of strongly confined surface plasmon polaritons in silver nanowires. Nano Letters. 2014;**14**(6):3628-3633

[32] Evans CI, Zolotavin P, Alabastri A, Yang J, Nordlander P, Natelson D. Quantifying remote heating from propagating surface plasmon polaritons. Nano Letters. 2017;**17**(9):5646-5652

[33] Zhang D, Xiang Y, Chen J, Cheng J, Zhu L, Wang R, Zou G, Wang P, Ming H, Rosenfeld M, Badugu R, Lakowicz JR. Extending the propagation distance of a silver nanowire plasmonic waveguide with a dielectric multilayer substrate. Nano Letters. 2018;**18**(2):1152-1158

[34] Zhuo X, Yip HK, Ruan Q, Zhang T, Zhu X, Wang J, Lin H-Q, Xu J-B, Yang Z. Broadside nanoantennas made of single silver nanorods. ACS Nano. 2018;**12**(2):1720-1731

[35] Shimizu K, Woo W, Fisher B, Eisler H, Bawendi MG. Surface-enhanced emission from single semiconductor nanocrystals. Physical Review Letters. 2002;**89**(11):117401

[36] Pompa P, Martiradonna L, Della Torre A, Della Sala F, Manna L, De Vittorio M, Calabi F, Cingolani R, Rinaldi R. Metal-enhanced fluorescence of colloidal nanocrystals with nanoscale control. Nature Nanotechnology. 2006;**1**(2):126

[37] Hong G, Tabakman SM, Welsher K, Wang H, Wang X, Dai H. Metal-enhanced fluorescence of carbon nanotubes. Journal of the American Chemical Society. 2010;**132**(45):15920-15923

[38] Geddes CD. Metal-enhanced fluorescence. Physical Chemistry Chemical Physics. 2013; **15**(45):19537-19537

[39] Sorokin AV, Zabolotskii AA, Pereverzev NV, Bespalova II, Yefimova SL, Malyukin YV, Plekhanov AI. Metal-enhanced fluorescence of pseudoisocyanine J-aggregates formed

in layer-by-layer assembled films. The Journal of Physical Chemistry C. 2015;**119**(5): 2743-2751

[40] Kim JK, Jang D-J. Metal-enhanced fluorescence of gold nanoclusters adsorbed onto Ag@ SiO$_2$ core-shell nanoparticles. Journal of Materials Chemistry C. 2017;**5**(24):6037-6046

[41] Yang X, Xu R, Bao D, Li B. Gold nanorod-enhanced light emission in quantum-dot-doped polymer nanofibers. ACS Applied Materials & Interfaces. 2014;**6**(15):11846-11850

[42] Bardhan R, Grady NK, Cole JR, Joshi A, Halas NJ. Fluorescence enhancement by Au nanostructures: Nanoshells and nanorods. ACS Nano. 2009;**3**(3):744-752

[43] Cohen-Hoshen E, Bryant GW, Pinkas I, Sperling J, Bar-Joseph I. Exciton-plasmon interactions in quantum dot-gold nanoparticle structures. Nano Letters. 2012;**12**(8):4260-4264

[44] Gueroui Z, Libchaber A. Single-molecule measurements of gold-quenched quantum dots. Physical Review Letters. 2004;**93**(16):166108

[45] Pons T, Medintz IL, Sapsford KE, Higashiya S, Grimes AF, English DS, Mattoussi H. On the quenching of semiconductor quantum dot photoluminescence by proximal gold nanoparticles. Nano Letters. 2007;**7**(10):3157-3164

[46] Pyayt AL, Wiley B, Xia Y, Chen A, Dalton L. Integration of photonic and silver nanowire plasmonic waveguides. Nature Nanotechnology. 2008;**3**(11):660-665

[47] Ditlbacher H, Hohenau A, Wagner D, Kreibig U, Rogers M, Hofer F, Aussenegg FR, Krenn JR. Silver nanowires as surface plasmon resonators. Physical Review Letters. 2005;**95**(25):257403

[48] Sanders AW, Routenberg DA, Wiley BJ, Xia Y, Dufresne ER, Reed MA. Observation of plasmon propagation, redirection, and fan-out in silver nanowires. Nano Letters. 2006; **6**(8):1822-1826

[49] Knight MW, Grady NK, Bardhan R, Hao F, Nordlander P, Halas NJ. Nanoparticle-mediated coupling of light into a nanowire. Nano Letters. 2007;**7**(8):2346-2350

[50] Akimov AV, Mukherjee A, Yu CL, Chang DE, Zibrov AS, Hemmer PR, Park H, Lukin MD. Generation of single optical plasmons in metallic nanowires coupled to quantum dots. Nature. 2007;**450**:402

[51] Fedutik Y, Temnov V, Woggon U, Ustinovich E, Artemyev M. Exciton-plasmon interaction in a composite metal-insulator-semiconductor nanowire system. Journal of the American Chemical Society. 2007;**129**(48):14939-14945

[52] Huang Y, Duan X, Wei Q, Lieber CM. Directed assembly of one-dimensional nanostructures into functional networks. Science. 2001;**291**(5504):630-633

[53] Yan R, Gargas D, Yang P. Nanowire photonics. Nature Photonics. 2009;**3**(10):569-576

[54] Yang X, Bao D, Li B. Light transfer from quantum-dot-doped polymer nanowires to silver nanowires. RSC Advances. 2015;**5**(75):60770-60774

[55] Lee S-Y, Park J, Kang M, Lee B. Highly efficient plasmonic interconnector based on the asymmetric junction between metal-dielectric-metal and dielectric slab waveguides. Optics Express. 2011;**19**(10):9562-9574

[56] Shegai T, Miljkovic VD, Bao K, Xu H, Nordlander P, Johansson P, Käll M. Unidirectional broadband light emission from supported plasmonic nanowires. Nano Letters. 2011; **11**(2):706-711

[57] Yu H, Li B. Wavelength-converted wave-guiding in dye-doped polymer nanofibers. Scientific Reports. 2013;**3**:1674

[58] Dionne J, Sweatlock L, Atwater H, Polman A. Planar metal plasmon waveguides: Frequency-dependent dispersion, propagation, localization, and loss beyond the free electron model. Physical Review B. 2005;**72**(7):075-405

[59] Yan R, Pausauskie P, Huang J, Yang P. Direct photonic–plasmonic coupling and routing in single nanowires. Proceedings of the National Academy of Sciences. 2009;**106**(50): 21045-21050

[60] Seo M-K, Kwon S-H, Ee H-S, Park H-G. Full three-dimensional subwavelength high-Q surface-plasmon-polariton cavity. Nano Letters. 2009;**9**(12):4078-4082

[61] Kang J-H, No Y-S, Kwon S-H, Park H-G. Ultrasmall subwavelength nanorod plasmonic cavity. Optics Letters. 2011;**36**(11):2011-2013

[62] Zhu QZ, Zheng SP, Lin SJ, Liu TR, Jin CJ. Polarization-dependent enhanced photoluminescence and polarization-independent emission rate of quantum dots on gold elliptical nanodisc arrays. Nanoscale. 2014;**6**(13):7237-7242

[63] Yang X, Bao D, Li B. Plasmon-mediated whispering-gallery-mode emission from quantum-dot-coated gold nanosphere. The Journal of Physical Chemistry C. 2015;**119**(45): 25476-25481

[64] Chikkaraddy R, de Nijs B, Benz F, Barrow SJ, Scherman OA, Rosta E, Demetriadou A, Fox P, Hess O, Baumberg JJ. Single-molecule strong coupling at room temperature in plasmonic nanocavities. Nature. 2016;**535**:127

[65] Shalabney A, George J, Hutchison J, Pupillo G, Genet C, Ebbesen TW. Coherent coupling of molecular resonators with a microcavity mode. Nature Communications. 2015;**6**:5981

[66] Noginov MA, Zhu G, Belgrave AM, Bakker R, Shalaev VM, Narimanov EE, Stout S, Herz E, Suteewong T, Wiesner U. Demonstration of a spaser-based nanolaser. Nature. 2009;**460**:1110

[67] Cerdán L, Enciso E, Martín V, Banuelos J, López-Arbeloa I, Costela A, García-Moreno I. FRET-assisted laser emission in colloidal suspensions of dye-doped latex nanoparticles. Nature Photonics. 2012;**6**(9):621626

[68] Yu J, Cui Y, Xu H, Yang Y, Wang Z, Chen B, Qian G. Confinement of pyridinium hemicyanine dye within an anionic metal-organic framework for two-photon-pumped lasing. Nature Communications. 2013;**4**:2719

[69] Huang KC, Seo M-K, Sarmiento T, Huo Y, Harris JS, Brongersma ML. Electrically driven subwavelength optical nanocircuits. Nature Photonics. 2014;**8**(3):244-249

[70] Shi C, Soltani S, Armani AM. Gold nanorod plasmonic upconversion microlaser. Nano Letters. 2013;**13**(12):5827-5831

[71] Lv Y, Li Y, Li J, Yan Y, Yao J, Zhao Y. All-color subwavelength output of organic flexible microlasers. Journal of the American Chemical Society. 2017;**139**:11329-11332

[72] Yang X, Li Y, Lou Z, Chen Q, Li B. Optical energy transfer from photonic nanowire to plasmonic nanowire. ACS Applied Energy Materials. 2018;**1**(2):278-283

[73] Wu X, Xiao Y, Meng C, Zhang X, Yu S, Wang Y, Yang C, Guo X, Ning C, Tong L. Hybrid photon-plasmon nanowire lasers. Nano Letters. 2013;**13**(11):5654-5659

[74] Miyata M, Takahara J. Colloidal quantum dot-based plasmon emitters with planar integration and long-range guiding. Optics Express. 2013;**21**(7):7882-7890